

## Drastic Reduction of Plasmon Damping in Gold Nanorods

C. Sönnichsen, T. Franzl, T. Wilk, G. von Plessen,\* and J. Feldmann

*Photonics and Optoelectronics Group, Physics Department and CeNS, University of Munich, D-80799 München, Germany*

O. Wilson and P. Mulvaney

*School of Chemistry, University of Melbourne, Parkville, 3010, Victoria, Australia*

(Received 9 August 2001; published 31 January 2002)

The dephasing of particle plasmons is investigated using light-scattering spectroscopy on individual gold nanoparticles. We find a drastic reduction of the plasmon dephasing rate in nanorods as compared to small nanospheres due to a suppression of interband damping. The rods studied here also show very little radiation damping, due to their small volumes. These findings imply large local-field enhancement factors and relatively high light-scattering efficiencies, making metal nanorods extremely interesting for optical applications. Comparison with theory shows that pure dephasing and interface damping give negligible contributions to the total plasmon dephasing rate.

DOI: 10.1103/PhysRevLett.88.077402

PACS numbers: 78.67.Bf, 73.22.Lp, 78.66.Vs

The collective oscillation of conduction electrons in metal nanoparticles is known as surface plasmon or particle plasmon. Strong light absorption and scattering, and considerable local-field enhancements, occur at the resonance frequency of the particle plasmon as a consequence of the large optical polarization associated with the collective electron oscillation [1]. These properties are of great interest for a range of optical applications, including surface-enhanced Raman scattering (SERS) spectroscopy [2,3].

Applications of particle plasmons often benefit from a weak plasmon damping, i.e., a slow dephasing of the optical polarization associated with the electron oscillation [4]. The processes leading to this damping have been the subject of extensive research and debate [1, 4–14]. The speed of the dephasing is characterized by the time constant  $T_2$ , which is related to the time constant for inelastic decay of the plasmon population,  $T_1$ , via  $T_2^{-1} = T_1^{-1}/2 + T^{*-1}$ , where  $T^*$  describes possible elastic phase-loss processes of the plasmon [5]. As shown schematically in Fig. 1, the population decay occurs via transformation of particle plasmons into photons (radiation damping) and via nonradiative decay into electron-hole excitations. The latter fall into two categories: *intraband* excitations within the conduction band and *interband* excitations due to transitions between other bands (e.g., the *d* bands of noble metals) and the conduction band. The mechanisms by which the decay into electron-hole excitations is linked to the scattering of individual electrons are a matter of debate; e.g., electron scattering off the particle surface and interaction with adsorbates may result in contributions to the decay called *interface damping*, which have been studied in [1,6]. One important open question that is rarely discussed is whether the dephasing of the polarization is caused by population decay only, or whether additionally some elastic phase-loss process of the collective excitation may contribute such that  $T^{*-1} \neq 0$ . Such *pure dephasing* processes have been reported for image-potential states at metal surfaces and

excitons in semiconductor quantum dots [15,16], where they are induced by elastic scattering of these excitations off phonons and static disorder.

Optical applications of metal nanoparticles, such as SERS, often require that the dephasing of the particle plasmon be as slow as possible [4]. In particular, it is advantageous to minimize the nonradiative decay, e.g., to avoid sample heating or quenching of fluorescence from adsorbed molecules; in other words, it is useful to maximize the quantum efficiency for resonant light scattering,  $\eta = T_{1,r}^{-1}/T_1^{-1} = T_{1,r}^{-1}/(T_{1,r}^{-1} + T_{1,nr}^{-1})$ , where  $T_{1,r}^{-1}$  and  $T_{1,nr}^{-1}$  are the rates for radiative and nonradiative population decay, respectively.

Because of its central importance for the fundamental understanding of particle plasmons as well as for optical applications, a number of experiments have been performed to measure the dephasing time  $T_2$  or homogeneous linewidth  $\Gamma = 2\hbar/T_2$  of the particle plasmon [4–7,13,14]. However, the  $T_2$  times reported so far vary widely for particles of the same metal. These variations may be partially due to differences in particle size and shape and possibly to inhomogeneous broadening effects present in experiments

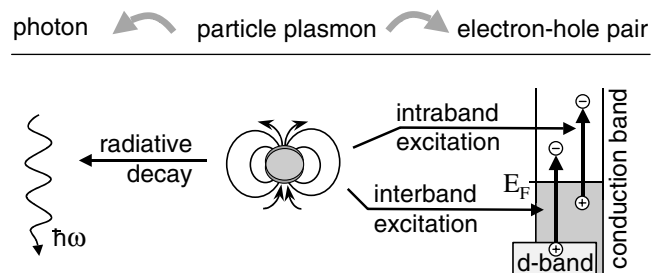


FIG. 1. Schematic representation of radiative (left) and nonradiative (right) decay of particle plasmons in noble-metal nanoparticles. The nonradiative decay occurs via excitation of electron-hole pairs either within the conduction band (intraband excitation) or between the *d* band and the conduction band (interband excitation).

on particle ensembles, and have made a systematic comparison with theory difficult.

In this Letter we systematically study the dephasing of particle plasmons in gold nanoparticles as a function of particle size and shape. We determine the homogeneous linewidth  $\Gamma$  of the plasmon resonance by spectrally investigating the light scattered by *single* particles, and we derive from  $\Gamma$  the dephasing time  $T_2$ . This approach avoids the problem of inhomogeneous broadening of the plasmon resonance frequencies. We find a drastic reduction of the plasmon dephasing rate in nanorods as compared to small nanospheres due to the suppression of the decay into interband excitations. The rods studied here also show very little radiation damping. Our results allow us to draw important conclusions about the local-field enhancement factors, light-scattering efficiencies, pure dephasing, and interface damping rates.

The particles investigated here were produced chemically. Nanospheres produced by reduction of a gold salt were obtained commercially in various sizes (diameters  $d = 20, \dots, 150$  nm) and with relatively narrow size distributions (size deviation  $<15\%$ ) [17]. Nanorods were prepared as described by Chang *et al.* [18] with a few modifications; full details are provided elsewhere [19]. The rods have diameters of  $b = 15\text{--}25$  nm along the two short axes and lengths of up to  $a = 100$  nm; thus they cover a large range of aspect ratios  $a/b$  but have much smaller volumes than any of the large spheres. Transmission electron microscope (TEM) images of a dense ensemble of rods and a single sphere are shown in Fig. 2 (bottom right). Both types of particles are monocrystalline and stored in stable suspensions in water. We spin cast a dilute suspension onto cleaned glass slides. After drying, we cover the slide with index matching fluid to ensure a homogeneous refractive index ( $n = 1.5$ ) around the particles.

The particles are investigated in a conventional microscope using a high aperture dark-field condenser, an oil im-

mersion objective, and a halogen lamp as the light source (Fig. 2, inset upper left). Individual nanoparticles can clearly be distinguished with this setup, as demonstrated by the true color photograph of a sample of gold nanorods (red) and nanospheres (green) in Fig. 2. Each bright spot corresponds to light scattered by an individual particle. For spectral investigations, the scattered light from single particles is focused with the microscope onto the entrance slit of a spectrometer coupled to a sensitive cooled CCD camera [13]. This dark-field spectroscopic technique allows us to record spectra with very little background light.

Typical single-particle scattering spectra from a nanosphere and a nanorod are shown in Fig. 3a. The spectra show the particle-plasmon resonances of the sphere at 2.19 eV and of the long-axis mode of the rod at 1.82 eV. The latter resonance is selected by using excitation light polarized along the long rod axis (in our samples, this axis is always oriented parallel to the sample surface). Figure 3b shows that the scattered-light intensity from this resonance follows the polarization-angle dependence expected for a perfect dipole. The short-axis resonance can be excited with light polarized along the short axis (not shown here). In the following, we will concentrate on the long-axis mode, which has a much higher oscillator strength and a lower resonance energy [1,9].

To investigate the plasmon resonances systematically, we extract the linewidths  $\Gamma$  and peak positions  $E_{\text{res}}$  of the plasmon peak from the spectra taken on nanospheres of various diameters  $d$  and nanorods of various aspect ratios  $a/b$ . The results of this analysis are shown in Fig. 4a, where  $\Gamma$  is plotted against  $E_{\text{res}}$ ; the right-hand scale shows the dephasing time deduced from  $\Gamma$  via  $T_2 = 2\hbar/\Gamma$ . The plasmon resonance of the spheres experiences a redshift with increased size due to increased electromagnetic retardation [1,9], while the wide variation in  $E_{\text{res}}$  observed for the rods results from the shape-induced redshift of the long-axis plasmon resonance known for elongated particles [1,9,18]. In this sense, the resonance energy plotted in Fig. 4a is a useful measure of the particle diameter and the aspect ratio. We note that the experimental accuracy

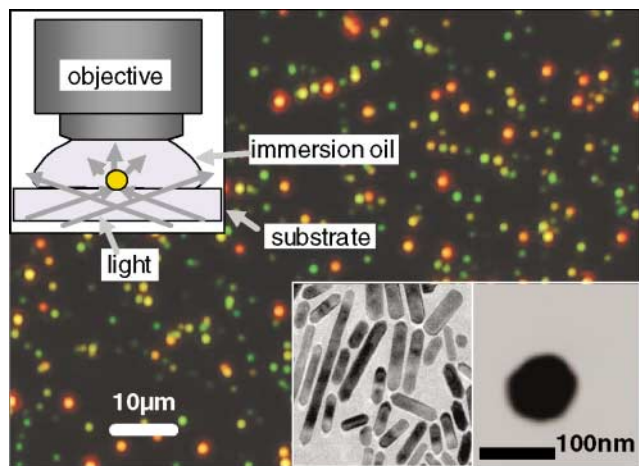


FIG. 2 (color). True color photograph of a sample of gold nanorods (red) and 60 nm nanospheres (green) in dark-field illumination (inset upper left). Bottom right: TEM images of a dense ensemble of nanorods and a single nanosphere.

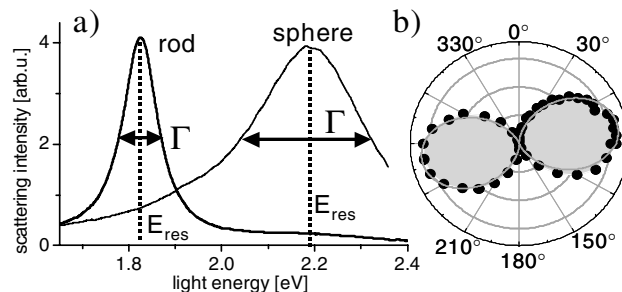


FIG. 3. (a) Light-scattering spectra from a gold nanorod and a 60 nm gold nanosphere measured under identical conditions (light polarized along the long rod axis). The resonance energies  $E_{\text{res}}$  and linewidths  $\Gamma$  are indicated. (b) Polar plot of the intensity from the long-axis plasmon resonance of a nanorod as a function of polarization angle of the exciting light. Dots: experimental data; line: dipole characteristic.

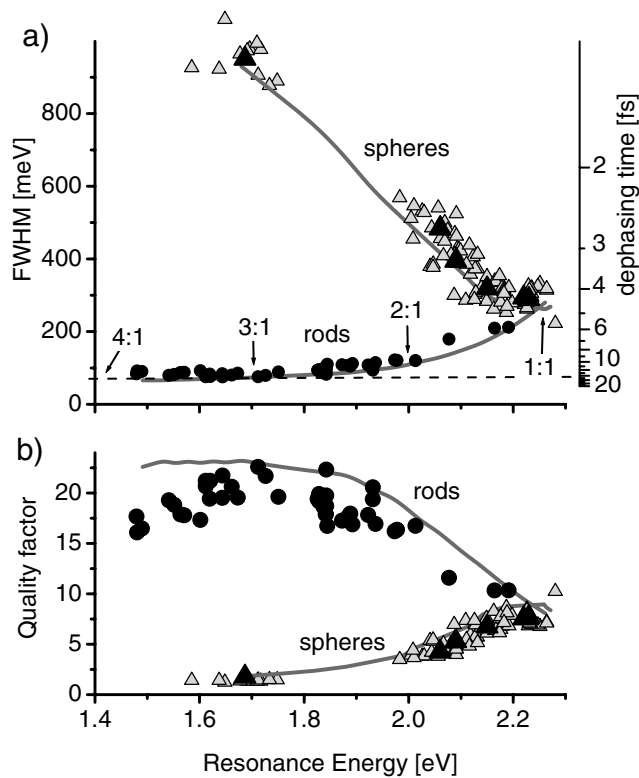


FIG. 4. (a) Measured linewidth  $\Gamma$  of plasmon resonances in single nanorods (dots) and nanospheres (open triangles) vs resonance energy  $E_{\text{res}}$ . The right scale gives the dephasing times  $T_2$  calculated from  $\Gamma$ . Black triangles: averages for spherical particles of the same nominal size (150, 100, 80, 60, 40, and 20 nm from left to right). Lines: theory. Some selected aspect ratios  $a/b$  are indicated. (b) Same data plotted as quality factor  $Q = E_{\text{res}}/\Gamma$ .

is better than the symbol size, i.e., the apparent distributions of  $E_{\text{res}}$  and  $\Gamma$  around the general trend are due to intrinsic sample properties. These distributions are possibly caused by small variations in the particle environment due to contamination on a molecular scale, charges in or on the particles, or to the faceting of the particle surfaces.

As shown in Fig. 4a, the particle-plasmon dephasing times  $T_2$  deduced from the experiment range from 1.4 to 5 fs for nanospheres and from 6 to 18 fs for nanorods. In the following, we will discuss the dependence of the dephasing rate  $T_2^{-1}$  on particle size and aspect ratio. In the case of the spheres, this dependence becomes clearer when the averages of the data for spheres of the same nominal diameter are marked (black triangles in Fig. 4a). The dephasing rate of nanospheres increases for more redshifted, i.e., larger, particles, which is explained by the increase of radiation damping expected for increased particle volume [2,13]. In contrast, the dephasing rate of nanorods *decreases* drastically with increasing redshift, i.e., for higher aspect ratios  $a/b$ . The limiting value of approximately  $T_2^{-1} = (18 \text{ fs})^{-1}$  is the smallest plasmon dephasing rate reported for gold nanoparticles to date. This surprising reduction of  $T_2^{-1}$  must be due to a reduced *nonradiative*

plasmon decay in the nanorods; it cannot be caused by a reduction in the *radiative* decay rate since the contribution of the latter decay mechanism is small for particles of small volume. For example, only 1.5% of the total damping rate in  $d = 20$  nm spheres is due to radiative decay, as estimated by Mie scattering theory [1]. The reduced non-radiative decay in nanorods is explained by the fact that interband excitations (cf. Fig. 1) require a threshold energy of about 1.8 eV in gold [20]; thus the process of plasmon decay into such interband excitations (which we will call *interband damping* [21] in the following) is precluded for plasmons with  $E_{\text{res}}$  below 1.8 eV. Of course, this suppression of interband damping should also be present in nanospheres with low  $E_{\text{res}}$ . However, the increase of *radiative* damping apparently outweighs this effect by far, resulting in much larger total linewidths in the spheres.

A more detailed picture of the plasmon decay process is gained by comparison with the results of theoretical calculations shown as solid lines in Fig. 4. The line through the nanosphere data is the result of an exact electrodynamic (Mie-theory [1]) calculation of particle-plasmon spectra for various sphere diameters  $d$ . The line along the nanorod data is the result of a simple quasistatic calculation of long-axis plasmon spectra of spheroidal nanoparticles for various aspect ratios  $a/b$  according to Eq. 2.31a of Ref. [1]. We use for our calculations the bulk dielectric function of gold measured on gold films under high vacuum conditions [20]; no further parameters enter the calculation. The agreement with the experiment is very good. In particular, the calculations reproduce the increased radiation damping for large spheres and the suppression of interband damping observed for nanorods of high aspect ratio  $a/b$ . Since the calculations for the rods disregard radiation damping, the good agreement confirms our above expectation that the contribution of this dephasing process is small in the rods. Furthermore, since the calculations neglect all surface effects, we conclude that interface damping effects are negligible in our samples. This is contrary to expectation; a straightforward extension of the usual treatment of interface damping [6] to the rod geometry predicts a considerable electron surface-scattering contribution to the damping, such that the maximum dephasing time of  $T_2 = 18$  fs observed here should be reduced to  $T_2 \approx 12$  fs for a surface-scattering parameter of  $A = 0.5$ . Another important conclusion can be drawn from the fact that the calculations contain no *pure dephasing* processes of the collective excitation; the good agreement between theory and experiment therefore implies that such processes, if they exist at all for particle plasmons, are negligible in our case, and the simple relation  $T_1 = T_2/2$  can be used.

We will now give an estimate of the radiative and non-radiative decay rates. In the dipolar approximation [2], the dependence of the radiative dephasing rate on particle volume is, for fixed  $E_{\text{res}}$ , given by  $T_{2,r}^{-1} = \kappa V$ , where  $\kappa$  is a constant. The rate of *nonradiative* dephasing of spheres

of a given size should be essentially equal to that of rods with the same resonance energy  $E_{\text{res}}$ ; thus the total dephasing rate of the spheres should differ from that of rods with the same  $E_{\text{res}}$  by an amount  $\Delta T_2^{-1} \approx \Delta T_{2,r}^{-1} = \kappa \Delta V$ , where  $\Delta V$  is the volume difference of the spheres and rods. Hence  $\kappa \approx \Delta T_2^{-1} / \Delta V$ ; from the data in Fig. 4a and estimates for  $\Delta V$ , we obtain  $\kappa \approx 4 \times 10^{-7} \text{ fs}^{-1} \text{ nm}^{-3}$ . This value can now be used in the above relation  $T_{2,r}^{-1} = \kappa V$  to estimate the radiative dephasing rate; for example, we obtain  $T_{2,r}^{-1} \approx (160 \text{ fs})^{-1}$  for rods with  $a/b = 3:1$  and  $b = 20 \text{ nm}$ . The *nonradiative* dephasing rate of these rods is then  $T_{2,nr}^{-1} = T_2^{-1} - T_{2,r}^{-1} = (18 \text{ fs})^{-1}$ , where the average  $T_2 = 16 \text{ fs}$  of the data from rods with low  $E_{\text{res}}$  was used. Using the relation  $T_1^{-1} = 2T_2^{-1}$ , we obtain a non-radiative population decay time of  $T_{1,nr} = 9 \text{ fs}$ . We note that the good agreement of this time with the Drude relaxation time of 9.3 fs determined in [20] confirms that the nonradiative decay of the particle plasmon in rods with low  $E_{\text{res}}$  is controlled by the relaxation of the intraband electron-hole excitations, as expected from the Drude-Lorentz-Sommerfeld model [1] for the quasifree electrons of a metal.

Using again the relation  $T_1^{-1} = 2T_2^{-1}$  to translate the (measured) total and (estimated) radiative dephasing rates into the respective population decay rates  $T_1^{-1}$  and  $T_{1,r}^{-1}$ , the quantum efficiency for resonant light scattering,  $\eta = T_{1,r}^{-1} / T_1^{-1}$ , can be calculated. For example, we obtain  $\eta \approx 10\%$  for rods with  $a/b = 3:1$  and  $b = 20 \text{ nm}$ . This value is considerably higher than the value of  $\eta \approx 3\%$  that would be expected for a sphere of the same volume. This higher quantum efficiency is a consequence of the reduced nonradiative decay due to the suppressed interband damping of the rod plasmons, and is consistent with our observation that the rods appear as bright in the microscopic measurement as spheres of much larger volume (cf. Figs. 2 and 3a). This high  $\eta$  could be further increased by enlarging the nanorod volume and thus increasing the radiative decay rate  $T_{1,r}^{-1}$ . We note that a high  $\eta$  should be very useful for optical applications where absorptive losses, sample heating, or quenching of fluorescence from adsorbed molecules need to be avoided.

Another important quantity follows immediately from the results in Fig. 4a, the quality factor of the resonance  $Q = E_{\text{res}} / \Gamma$ . The quality factor is the enhancement of the oscillation amplitude of a driven oscillating system with respect to the driving amplitude, i.e., the local-field enhancement in the case of particle plasmons. This value is a figure of merit for all nonlinear applications of particle plasmons such as SERS, which is believed to be proportional to  $Q^4$  [3,22]. The quality factors for the particles studied here are shown in Fig. 4b. It is clear from this plot that spherical gold particles have relatively low-field enhancement factors; this is a consequence of interband damping for small spheres and radiation damping for large spheres [2]. In contrast, gold nanorods can have very high quality factors of up to 23 due to the suppressed interband

damping (the slight decrease of  $Q$  below 1.7 eV is due to the decrease of  $E_{\text{res}}$ ). These high quality factors should make gold nanorods vastly superior to gold nanospheres in optical applications where large local-field enhancements are required, such as SERS.

In conclusion, we have investigated the dephasing of particle plasmons in single gold nanoparticles. We have found a drastic reduction of the plasmon dephasing rate in nanorods as compared to small nanospheres due to the suppression of interband damping. As compared to large nanospheres, the rods studied here show much weaker radiation damping, due to their small volumes. These findings result in relatively high light-scattering efficiencies and large local-field enhancement factors, making nanorods interesting for a range of optical applications. Comparison of our experimental results with theory shows that interface damping and pure dephasing, i.e., collective dephasing without plasmon-population decay, give negligible contributions to the total plasmon dephasing rate.

We thank Martin Barradine [17] for TEM images of nanospheres. Support by the DFG through the SFB 486, PI261/2-2, and the Leibniz Award, and by the EU through the "Ultrafast Quantum Optoelectronics" TMR network is acknowledged.

\*Present address: I. Phys. Inst., RWTH Aachen, D-52056 Aachen, Germany.

- [1] U. Kreibig and M. Vollmer, *Optical Properties of Metal Clusters* (Springer, Berlin, 1995).
- [2] A. Wokaun, J. P. Gordon, and P. F. Liao, *Phys. Rev. Lett.* **48**, 957 (1982).
- [3] K. Kneipp *et al.*, *Phys. Rev. Lett.* **78**, 1667 (1997).
- [4] T. Klar *et al.*, *Phys. Rev. Lett.* **80**, 4249 (1998).
- [5] E. J. Heilweil and R. M. Hochstrasser, *J. Chem. Phys.* **82**, 4762 (1985), and references therein.
- [6] H. Hövel *et al.*, *Phys. Rev. B* **48**, 18 178 (1993).
- [7] B. Lamprecht, A. Leitner, and F. R. Aussenegg, *Appl. Phys. B* **64**, 269 (1997); **68**, 419 (1999).
- [8] R. Schlipper *et al.*, *Phys. Rev. Lett.* **80**, 1194 (1998).
- [9] S. Link and M. A. El-Sayed, *J. Phys. Chem. B* **103**, 8410 (1999).
- [10] T. V. Shahbazyan and I. E. Perakis, *Phys. Rev. B* **60**, 9090 (1999).
- [11] F. Stietz *et al.*, *Phys. Rev. Lett.* **84**, 5644 (2000).
- [12] J. Lehmann *et al.*, *Phys. Rev. Lett.* **85**, 2921 (2000).
- [13] C. Sönnichsen *et al.*, *Appl. Phys. Lett.* **77**, 2949 (2000).
- [14] Y.-H. Liao *et al.*, *J. Phys. Chem. B* **105**, 2135 (2001).
- [15] X. Fan *et al.*, *Solid State Commun.* **108**, 857 (1998).
- [16] Ch. Reuss *et al.*, *Phys. Rev. Lett.* **82**, 153 (1999).
- [17] BBInternational, Golden Gate, TY Glas Ave., Cardiff CF4 5DX, United Kingdom.
- [18] S.-S. Chang *et al.*, *Langmuir* **15**, 701 (1999).
- [19] O. Wilson *et al.* (to be published).
- [20] P. B. Johnson and R. W. Christy, *Phys. Rev. B* **6**, 4370 (1972).
- [21] B. Bernert and P. Zacharias, *Z. Phys. A* **241**, 205 (1971).
- [22] V. M. Shalaev, E. Y. Poliakov, and V. A. Markel, *Phys. Rev. B* **53**, 2437 (1996).